VII International Conference on Computational Methods for Coupled Problems in Science and Engineering
COUPLED PROBLEMS 2017
M. Papadrakakis, E. Oñate and B. Schrefler (Eds)

ON FORWARD AND REVERSE COUPLING OF VIBRATING PIEZOELECTRIC ENERGY HARVESTERS

ELVIO BONISOLI*, NICOLÓ MANCA+ AND MAURIZIO REPETTO†

*Department of Mechanical and Aerospace Engineering (DIMEAS)
e-mail: elvio.bonisoli@polito.it - Web page: http://www.dimeas.polito.it/en/
+Department of Management and Production Engineering (DIGEP)
e-mail: nicolo.manca@polito.it - Web page: http://www.digep.polito.it/en/
†Department of Energy ≪Galileo Ferraris≫ (DENERG)
Politecnico di Torino, Corso Duca degli Abruzzi, 24, 10129 Torino, Italy
e-mail: maurizio.repetto@polito.it - Web page: http://www.cadema.polito.it

Key words: Piezoelectric materials, Energy harvesters, Vibrations

Abstract. This document provides information about the analysis of effects coupling the mechanical and the electrical phenomena going on inside a piezoelectric energy harvester. Two characteristics are exploited in energy harvesting: direct piezoelectric effect where stress is resulting by the application of an electric field and reverse effect showing an electric field resulting by stress application. Piezoelectric patches, bonded on beams free to vibrate under a mechanical stimulus, can be used as active elements. Point-wise material characteristics are described by symmetric matrices coupling together stress and electric field to the strain and the electric polarisation leading to reciprocal direct and reverse effects. Under operating conditions, the stress and electric field values applied to the material patch are not uniform and do not have the same spatial pattern resulting in a non reciprocal interaction. An explanation of this phenomenon is attempted by applying the Euler-Bernoulli beam theory model that allows the computation of two geometrical coefficients for direct and inverse interactions under uniform stress distribution. Comparisons versus experiments carried out on a Macro Fiber Composite piezoelectric patch show that the model is able to estimate the effect.

1 INTRODUCTION

PiezoElectricity (PE) phenomenon can be used as sensor if the stress applied to a sample can be measured by a voltage appearing on the material, or as actuator if the material changes its shape due to the application of a electric field. In energy harvesting applications both effects have to be exploited since power is converted from the mechanical action, as for instance mechanical vibrations, to the electrical domain when power is transferred to an external electric circuit. These effects are well known and have been

used to recover part of the vibration energy applied to the material in an external electrical circuit [1].

In all harvesting applications the estimation of the maximum power that can be extracted by some kind of excitation is of fundamental importance for the evaluation of potential applications. In this respect the accurate simulation of all the components present in the energy conversion chains is fundamental [2].

The energy conversion chain is composed by a direct effect where an elastic beam is set in motion by a vibrating source. This primary action creates stresses on the PE material and, in consequence, a voltage is generated. If an external circuit is connected to the voltage a power is drained and dynamic of the system is modified by the appearance of a force that is responsible for the power transferred from the mechanical to the electrical domain. These effects are called *direct effect* for the actions going from the mechanical to the electrical domain and *reverse effect* for the opposite.

If the vibrating beam is described by one degree of freedom, for instance the displacement of the free end from its equilibrium position, these two phenomena can be modelled by lumped parameters approach of the electromechanical model. Experimentally a non reciprocity of the energies exchanged by the two domains, mechanic and electric, is measured. To explain this fact an analysis of the actual stresses acting on the structure must be carried out and the model must be validated by experiments.

This paper is structured as: in the following chapter the analysis of the PE electromagnetic conversion is described while the following one deals with the experimental setup used to validate the model. Eventually a discussion of the obtained results is performed and the comparison with experiments is carried out.

2 PIEZOELECTRIC MATERIAL MODELLING

In energy harvesting applications, the piezoelectric effect can be described by using the linear constitutive equations of the piezoelectric materials [3]:

$$\begin{aligned} \boldsymbol{\delta_p} &= \boldsymbol{s^E} \cdot \boldsymbol{\sigma} + \boldsymbol{d}^T \cdot \boldsymbol{E} \\ \boldsymbol{D} &= \boldsymbol{d} \cdot \boldsymbol{\sigma} + \boldsymbol{\varepsilon^\sigma} \cdot \boldsymbol{E} \end{aligned} \tag{1}$$

where $\boldsymbol{\delta_p}$ is the mechanical strain, $\boldsymbol{\sigma}$ is the mechanical stress, $\boldsymbol{D}$ is the electrical displacement (charge density), $\boldsymbol{E}$ is the electric field, $\boldsymbol{s^E}$ is the compliance under a zero or constant electrical field (indicated by the superscript E) and $\boldsymbol{\varepsilon^\sigma}$ is the dielectric permittivity under a zero or constant stress (indicated by the superscript σ). $\boldsymbol{d}$ and $\boldsymbol{d}^T$ are the matrices for the direct and the reverse piezoelectric effect, where the superscript T means the transposed matrix. All matrices are (3×3) and express the anisotropy of the problem.

In the present application the PE material is exploited by applying a single axis stress, like in figure 1. As a result the constitutive equation (1) can be simplified in one dimension as:

$$\begin{aligned} \delta_1 &= s_{11}^E \cdot \sigma_1 + d_{31} \cdot E_3 \\ D_3 &= d_{31} \cdot \sigma_1 + \varepsilon_{33}^\sigma \cdot E_3 \end{aligned} \tag{2}$$

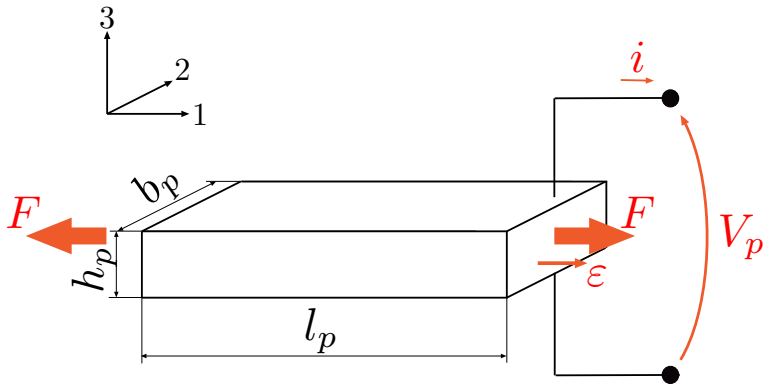

Figure 1: Layout of the PE harvester.

When a force F is applied along the 1 direction, it causes the elongation ϵ along the same direction. Due to the piezoelectric effect, a voltage V_p is generated in the 3 direction and, if a circuit is connected, a current i is created.

A lumped parameter model of the structure can be defined if, instead of considering equation (2), macroscopic variables F, ϵ, V_p and i are used. By taking into account geometric dimensions defined in figure 1, and considering that all quantities are uniform on the patch, the following relations can be written:

$$E_3 = -\frac{V_p}{h_p}\,; \qquad q = D_3 b_p l_p\,; \qquad \sigma_1 = \frac{F}{b_p h_p}\,; \qquad \delta_1 = \frac{\varepsilon}{l_p}\,; \qquad i = \frac{dq}{dt} \tag{3}$$

and, by substitution in eq. (2), the following dynamic equations are obtained:

$$\begin{cases} F = k_p \varepsilon + \Gamma V_p \\ i = \Gamma \dot{\varepsilon} - C_p \dot{V}_p - \frac{V_p}{R} \end{cases} \tag{4}$$

where:

$$k_p = \frac{b_p h_p}{l_p\, s_{11}^E}\,; \qquad C_p = \left(\varepsilon_{33}^\sigma - \frac{d_{31}^2}{s_{11}^E}\right)\frac{b_p l_p}{h_p}\,; \qquad \Gamma = \frac{d_{31} b_p}{s_{11}^E}$$

Eq. (4) has been derived from the constitutive equations of the piezoelectric material in static condition so that no mechanical dissipative effects are present. Even if, in the majority of cases, this effects are negligible at least in the modelling of the system it has to be considered. Thus, in dynamic conditions, the term $c_p\dot{\varepsilon}$ is added to the expression of F, where c_p is the mechanical damping of the piezoelectric patch.

3 BONDED PATCH DYNAMICS

The relations obtained in the previous section are the PE constitutive equations, that is they are relevant to the material characteristics. Being the PE patch bonded to an elastic beam the actual stress conditions applied to the material must be related to the macroscopic variables of the beam and to the average non-uniform stress conditions.

3.1 Relation between beam and PE variables

The clamped beam is free to move on one end and the relative vertical position z_r of the beam tip with respect to the clamped end is a quantity that can be measured. At the same time, due to the deformation of the beam, the PE patch is subject to an elongation ϵ that appears in the equation (4). In order to relate the two variables, the analysis of the one dimensional dynamic of the structure must be performed. As a result, the $1d$ model of the mechanical part will be defined in terms of the macroscopic variables $\dot{z}_r$ and F_T.

In a cantilever beam EH system, the piezoelectric force F acting on the patch along the 1 direction, due to the characteristics of the system, produces a force F_T applied to the free-end of the cantilever beam along the z axis. In the same way, the displacement of the free-end along the z axis, due to the characteristics of the system, induces elongation along the 1 direction of the piezoelectric patch.

3.1.1 direct effect: A coefficient

When voltage is applied at the piezoelectric patch along the 3 direction, a force F is produced along the 1 direction due to piezoelectric 31 effect. Being the patch neutral surface at a distance Δh along the 3 direction from the neutral surface of the support beam, the piezoelectric layer imposes a moment M to the support beam. The equilibrium of the system is achieved applying a force F_T at the free-end of the support beam creating a moment M_T that balances M, Fig. 2a.

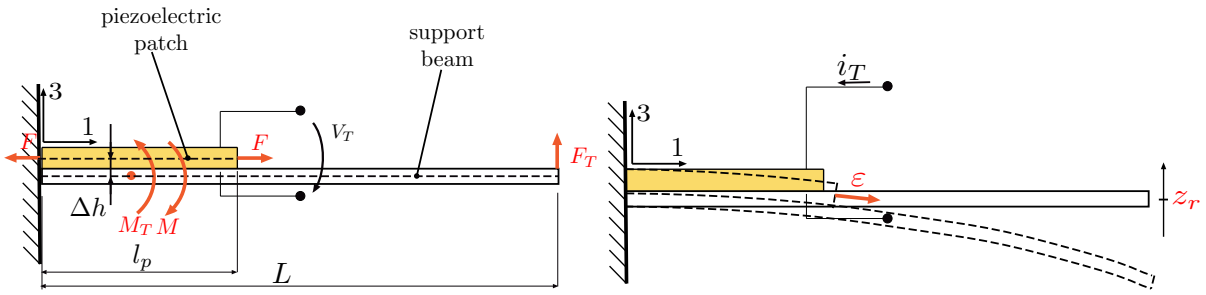

(a) (b)

Figure 2: Piezoelectric cantilever beam schemes for a) the calculation of A and b) B coefficients.

The coefficient that relates F and F_T is derived as follows.

$$M_T + M = 0 \tag{5}$$

$$F_T\big(L - \frac{l_p}{2}\big) + F\Delta h = 0 \tag{6}$$

$$F_T + \frac{\Delta h}{\big(L - \frac{l_p}{2}\big)}F = 0 \tag{7}$$

$$F_T = -\frac{\Delta h}{\big(L - \frac{l_p}{2}\big)}F = -AF \tag{8}$$

$$\Rightarrow A = \frac{\Delta h}{\big(L - \frac{l_p}{2}\big)} \tag{9}$$

where geometric variables are highlighted in figure 2a.

3.1.2 inverse effect: B coefficient

A displacement z imposed to the free-end of the piezoelectric beam induces a curvature to the neutral surface, see figure 2b. In the hypothesis that the mechanical properties of the piezoelectric material are negligible with respect to that of the support beam material, the neutral surface of the support beam is not shifted, the curvature $\frac{d^2 z_r}{dx^2}$ of the neutral surface of the cantilever beam loaded at the free end and its displacement are:

$$\frac{d^2 z_r}{dx^2} = \frac{F_T}{E_s I_s}(L - x) \tag{10}$$

$$z_r = \frac{L^3}{3E_s I_s}F_T \tag{11}$$

$$\Rightarrow \frac{d^2 z_r}{dx^2} = \frac{3}{L^3}z_r(L - x) \tag{12}$$

Being the patch at a distance Δh from the neutral surface of the support beam, strain is induced along the 1 direction. The average strain is obtained by integrating $\delta_1(x)$ along the PE patch:

$$\delta_1(x) = -\Delta h\frac{d^2 z_r}{dx^2} = -\Delta h\frac{3}{L^3}z_r(L - x) \tag{13}$$

$$\delta_1 = -\frac{3\Delta h\, z_r}{L^3}\frac{1}{l_p}\int_0^{l_p}(L - x)dx = -\frac{3\Delta h}{L^3}z_r\big(L - \frac{l_p}{2}\big) \tag{14}$$

The piezoelectric patch elongation is:

$$\varepsilon = l_p \delta_1 = -l_p \frac{3\Delta h}{L^3}\big(L - \frac{l_p}{2}\big) z_r = -B z_r \tag{15}$$

$$\Rightarrow B = l_p \frac{3\Delta h}{L^3}\big(L - \frac{l_p}{2}\big) \tag{16}$$

$$\tag{17}$$

3.2 Electromechanical PE equations in terms of beam variables

By the computation of the geometrical coefficients A and B it is now possible to relate the beam and the patch quantities as:

$$F_T = -AF \tag{18}$$

$$\dot{\epsilon} = -B\dot{z}_r \tag{19}$$

The coupling equations of the piezoelectric patch used in 31 mode, eq.(4), become the equations of the piezoelectric transducer consisting of a the patch bonded on a cantilever beam:

$$\begin{cases} F_T &= -A\,F = -A(c_p\dot{\varepsilon} + k_p\varepsilon + \Gamma V_T) = c_{p\_eq}\,\dot{z}_r + k_{p\_eq}\,z_r - \alpha V_T \\ i_T &= \Gamma\dot{\varepsilon} - C_p\dot{V}_T - \frac{V_T}{R} = -\beta\dot{z}_r - C_p\dot{V}_T - \frac{V_T}{R} \end{cases} \tag{20}$$

where coefficients are relevant to patch behaviour when it is referred to the relative displacement of the tip mass and are:

- F_T is the force acting on the tip mass along z direction due to the piezoelectric patch;
- $k_{p\_eq} = ABk_p$ is the equivalent mechanical stiffness;
- $c_{p\_eq} = ABc_p$ is the equivalent damping;
- i_T and V_T are the output current and voltage of the transducer;
- $\alpha = A\Gamma$ and $\beta = B\Gamma$ are the electromechanical coupling coefficients of the transducer respectively for the reverse and forward piezoelectric effect;
- C_p and R are the clamped capacitance and the dielectric loss respectively.

4 GOVERNING EQUATIONS OF THE SYSTEM

Equations (20) describe dynamics of the patch but are not taking into account the presence of the beam, whose mechanical characteristics must be considered in the overall behaviour of the system. The mass, damping and elastic parameters of the two bonded systems will be merged by considering that they are both contributing to the model simulations formulated in terms of z_r.

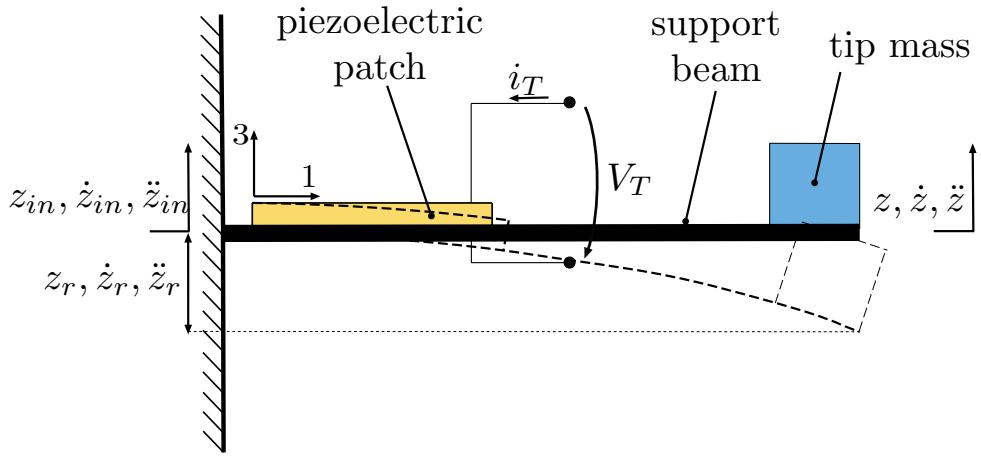

Figure 3: Structure of the vibrating harvester.

The complete simulated structure is outlined in figure 3 where a tip mass is added to enhance harvesting capabilities.

The parameters that must be combined together are:

- *system mass*: the overall mass is given by the combination of the mass m_p of the patch, m_s of the supporting beam and m_t of the tip mass. Since the position of the beam and patch are not coincident with that of the tip, a geometric coefficient θ is used to add them up correctly.

$$m = m_t + \theta(m_s + m_p) \tag{21}$$

- *system stiffness*: the overall stiffness of the mechanical system k_m is given by the contribution due to the bending stiffness k_s of the cantilever beam and the contribution due to the bonded piezoelectric patch k_p:

$$\begin{aligned} k_m &= k_s + k_{p\_eq} \\ k_s &= \tfrac{3E_sI_s}{L^3} \\ k_{p\_eq} &= A\,B\,k_p \end{aligned} \tag{22}$$

  where E_s is the elastic modulus of the cantilever beam and $I_s = \frac{b_s h_s^3}{12}$ is its second moment of inertia.

- *system damping*: the overall damping of the mechanical system c_m is given by the sum of the contribution of the cantilever beam c_s and the one of the piezoelectric patch c_p.

- *coupling electromechanical coefficients*: the two physical domains are coupled by the force due to the *electrical* effects $F_{el} = A\Gamma V_T = \alpha V_T$. Physical dimensions of α are N/V. The current generated by patch deformation along 1 direction is $i_p = B\Gamma\dot{z}_r = \beta\dot{z}_r$. Physical dimensions of β are As/m;

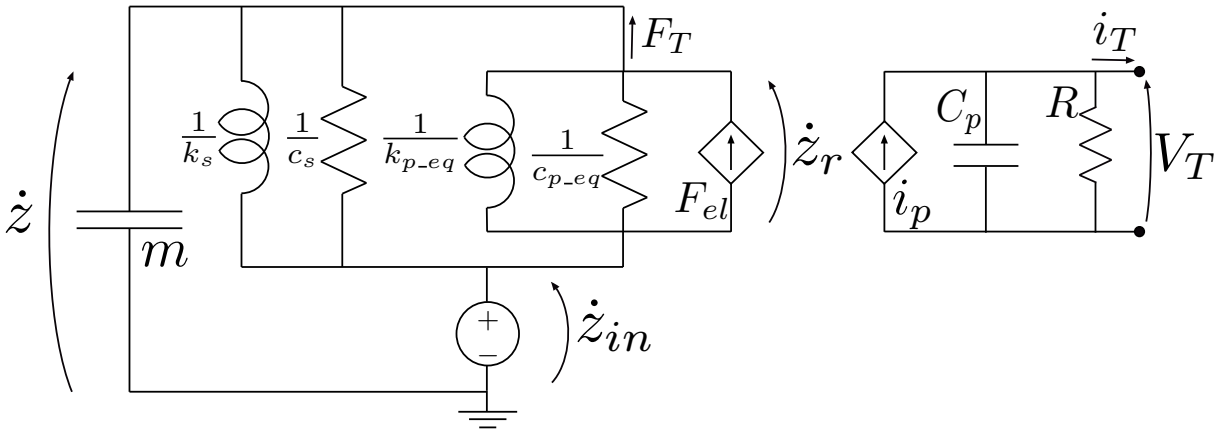

Figure 4: Equivalent circuit of the electromechanical conversion.

- *system excitation*: the system is free to vibrate when a displacement z_{in} is applied to the clamped end of the beam. The mass dynamic is written in terms of the relative position $z = z_r + z_{in} \Rightarrow m\ddot{z} = m\ddot{z}_r + m\ddot{z}_{in}$. The last term is known and can be considered as the forcing term of the equation [4].

The governing equations of the system can thus be written as

$$\begin{cases} m\ddot{z}_r + c_m\dot{z}_r + k_m z_r + F_{el} = -m\ddot{z}_{in} \\ i_T = i_p - C_p\dot{V}_T - \frac{V_T}{R} \end{cases} \tag{23}$$

4.1 Electromechanical circuit model

Using these assumptions the system dynamics can be described by the electromechanical circuit outlined in figure 4.

The dynamic of the mechanical part of the model is described in terms of the concept of *across* or *effort* variables and of *through* or *flow* variables. An across/effort variable is a variable determined by measuring the difference of values acting at the two extreme points of an element or in a specific point. A through/flow variable is a variable transmitted through an element without modification. The product of the two must be a power. By using the Firestones analogy, the mass m is substituted by a grounded capacitor $C = m$, and the spring k_m by an inductor $L = 1/k_m$. The inertial force imposed by the kinematics is substituted by a current source and the electric force by the transducer terminals [5].

The network is shown in open circuit conditions but a R_L load resistor can be connected at the terminals so that it is subject to the electric variables V_T and i_T.

4.2 Power considerations

By multiplying the first of eq. (23) by $\dot{z}_r$ and the second by V_T, the power balance of the mechanical part and of the electrical side is derived:

$$\begin{aligned} \underbrace{-m\ddot{z}_{in}\dot{z}_r}_{input} &= \underbrace{m\ddot{z}_r\dot{z}_r}_{kinetic} + \underbrace{c_m\dot{z}_r^2}_{damping} + \underbrace{k_m\dot{z}_r z_r}_{elastic} + \underbrace{(-\alpha V_T\dot{z}_r)}_{piezoelectric} \\ \underbrace{V_T i_T}_{output} &= \underbrace{(-\beta\dot{z}_r V_T)}_{converted} - \underbrace{C_p\dot{V}_T V_T}_{capacitance} - \underbrace{\frac{V_T^2}{R}}_{piezo\,losses} \end{aligned} \tag{24}$$

The input power of the system, namely the power extracted from the mechanical source and injected in the harvester, consists of the kinetic power of the floating mass, the elastic power stored in the mechanical spring, the power wasted through the mechanical damper and the overall power delivered to the the electric part of the system through the piezoelectric element. The output power, namely the electric power provided to the electrical part of the system, consists of the converted power from the mechanical domain minus the power stored in the clamped capacitance of the piezoelectric patch and that lost by the dielectric.

It is worth noting that the input power of the electrical part, the converted power, is different from the power outgoing the mechanical system due to the piezoelectric coupling. As $\alpha > \beta$, the input power in the electrical part, namely the maximum recoverable, is lower than the power outgoing the mechanical part.

The electromechanical coupling coefficients β and α describe how the transducer relates the mechanical variable $\dot{z}_r$ to the electrical variable i and how the electrical variable V_T is related to the mechanical variable F_{el}. β and α extend the meaning of Γ when a mechanical transformer is interposed between the vibrating system and the transducer piezoelectric patch. In this case the mechanical transformer is represented by the cantilever beam that relates the 1 direction of the piezoelectric patch to the 3 or z direction of the vibrating system through the coefficients A and B.

4.3 Behaviour in short and open circuit conditions

The behaviour of the system can be highlighted in two extreme operating conditions: if output terminals are short circuited the voltage V_T is null and so are the converted power and the direct effect. On the other hand if output terminals are left open all the power is transferred to the conservative element C_p and resulting in an increase system stiffness.

Considering open and short-circuit condition of the electric terminals of the transducer, Fig. 4, two different resonance frequencies exist.
In short circuit, V_T is null, thus no energy is transferred to the electric load and no electrical feedback force acts to the mechanical part. The resonance frequency of the

system depends only on its mechanical properties:

$$k_{SC} = k_m \omega_{SC} = \sqrt{\frac{k_{SC}}{m}} \tag{25}$$

In open circuit, i_T is null and V_T is in phase with z_r. Thus, the controlled force generator acts as a spring k_{el} or, according to the mobility analogy, it can be replaced with an inductor $\frac{C_p}{\alpha\beta}$. It follows a stiffer mechanical system:

$$k_{OC} = \frac{1}{L_{OC}} = k_{SC} + \frac{\alpha\beta}{C_p} > k \tag{26}$$

where an electric stiffness is defined as:

$$k_{el} = \frac{\alpha\beta}{C_p} \tag{27}$$

Higher resonance frequency results:

$$\omega_{OC} = \sqrt{\frac{k_{OC}}{m}} = \omega_{SC} \sqrt{1 + \frac{\alpha\beta}{k_{SC} C_p}} \tag{28}$$

It is worth noting that, in both open and short circuit conditions, the damping effect due to the electric load ($R_L = \infty$ and $R_L = 0$ respectively) is null.

5 EXPERIMENTAL VALIDATION

The model developed in the previous sections has been validated on an experimental setup and evaluation of the accuracy of direct and inverse coefficients has been checked.

5.1 Experimental setup

The support cantilever beam is a stainless steel beam which geometrical features are summarised in figure 5. The patch is 28 mm long and beam is 100 mm long, 25 mm wide, 0.5 mm tick, and consists of two parts: a clamped portion of 40 mm that is locked in the shaker fixture and a free portion of 60 mm that represents the effective oscillating elements. Considering standard stainless steel, $E_s = 180$ GPa, the first flexural mode occurs at 109 Hz.

The tip-mass is obtained clamping the free-end of the beam with two $\varnothing 15 \times 3$ mm magnets in attraction. It results a cylindrical shape mass of $7.95 \cdot 10^{-3}$ kg whose application point on the support beam, with respect to the free-end, is shifted half of the diameters toward the joint. It follows a shorter effective oscillating length of the support beam.
The first flexural mode of the system is at 56 Hz, that falls in the frequency range of interest.

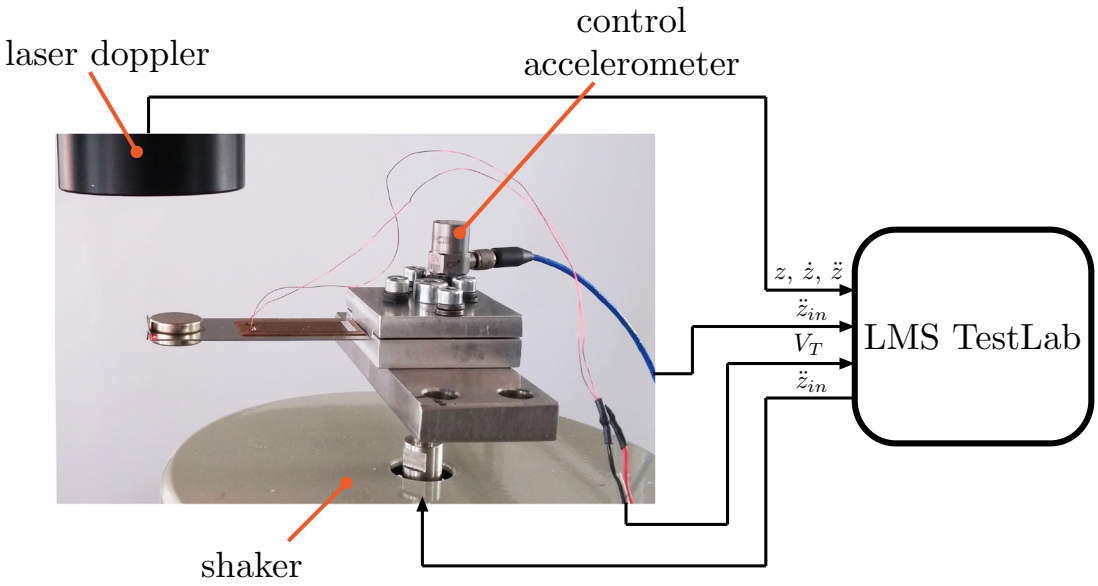

Figure 5: Experimental setup and measurement points connected to the external software *LMS TestLab*.

5.2 Experimental validation of the coupling coefficients

In order to assess experimentally the two coefficients of direct and inverse coupling, the structure is stressed in two extreme conditions: short and open circuit. These two operating conditions allow to highlight the power transfer between the two domains of the energy conversion.

The direct coupling coefficient β has been evaluated in steady state condition following the procedure proposed in [6]. A short circuit configuration is emulated by connecting the piezoelectric patch terminals to a low resistor, $R_L = 110.5\ \Omega$. The electrical feedback on the mechanical part αV_T is almost cancelled. The load resistor impedance is, in fact, at least two orders of magnitude lower than that of the clamped capacitance at the involved frequencies and, thus, the current through C_p is negligible. The induced current $\beta \dot{z}_r$ flows almost entirely through the load resistor so that:

$$i_T = \frac{V_T}{R_L} \cong \beta \dot{z}_r \ \Rightarrow \ \beta = \frac{V_T}{\dot{z}_r R_L} \tag{29}$$

Measuring the amplitude of the output voltage V_T and of the mass relative velocity $\dot{z}_r$, the direct coupling coefficient β is derived. Vibrating mechanical input is applied at the short circuit resonance frequency ω_{SC} considering two acceleration amplitude levels, 0.5 and 0.8 m/s^2. Two slightly different values derive for the direct coupling coefficient, but with relative difference lower than 3%. The mean value is considered and $\beta = 7.993\,10^{-4}$ As/m results.

The reverse coupling coefficient α has been evaluated considering the definition of k_{el},

eq. (27):

$$\alpha = \frac{C_p k_{el}}{\beta} \tag{30}$$

$\alpha = 8.353\,10^{-4}$ N/V results. A second evaluation of α has been performed considering static condition in order to cancel the direct piezoelectric effect. Constant voltage is applied to the transducer terminals. The first of eq. (23) becomes:

$$kz_r + \alpha V_T = 0 \;\Rightarrow\; \alpha = \frac{kz_r}{V_T} \tag{31}$$

and by measuring the mass displacement z_r at equilibrium, α is derived. When $V_T = 15$ V is applied, $z_r = 9.4447\,10^{-6}$ m is measured and $\alpha = 8.418\,10^{-4}$ N/V follows. The difference between the two values obtained for α results lower than 1%. The mean value $\alpha = 8.386\,10^{-4}$ N/V is considered. The ratio between the two values is:

$$\frac{\alpha}{\beta} = 1.049 \tag{32}$$

the ratio between α and β is a pure number.

By computing the geometrical coefficients A and B it is possible to evaluate the same ratio that turns out to be:

$$\frac{A}{B} = 1.162 \tag{33}$$

6 DISCUSSION

The evaluation of the direct and inverse effect of the piezoelectric energy conversion is important to evaluate the potential of energy harvesting. The asymmetry between direct and inverse effect is experimentally observed and its explanation is attempted by addressing the different stress conditions created by electric potential and strain. The direct effect, that is the strain created by the application of electric field, is in fact applying a distributed load on the beam, while the vibration is loading the beam at its tip. Different strain patterns arise and this is explained in terms of the Euler-Bernoulli beam theory. The model obtained is one dimensional as the only geometric variable is the relative tip elongation with respect to the clamped end z_r.

The theoretical model is evaluated versus a experimental mock-up and ratios between the computed and experimental direct and inverse coefficients are evaluated. The theoretical model is able to point out a difference between the α and β values but its estimate is larger than the one obtained experimentally.

This effect can be attributed to some restrictive hypotheses that have been adopted in the theoretical treatment. In particular the uniformity of stresses and properties within the PE patch are to be investigated in deeper details. Also boundary conditions of the bonded patch on the beam could be not ideal as supposed. These aspects will be investigated in future researches.

Acknowledgents

Authors would like to thank the help of the team of Prof. Lauric Garbuio of the Grenoble Institute of Technology (G2Elab) for the experimental activity on the piezoelectric arrangement.

References

[1] Thomas Daue and Jan Kunzmann. Energy harvesting systems using piezo-electric mfcs. In *2008 17th IEEE International Symposium on the Applications of Ferroelectrics*, volume 1, pages 1–1. IEEE, 2008.

[2] Elvio Bonisoli, Maurizio Repetto, Nicolo Manca, and Alessandro Gasparini. Electromechanical and electronic integrated harvester for shoes application. *IEEE/ASME Transactions on Mechatronics*, ¡not found¿(¡not found¿):1–12, 2017.

[3] Thorsten Hehn and Yiannos Manoli. *Piezoelectricity and Energy Harvester Modelling*, pages 21–40. Springer Netherlands, Dordrecht, 2015.

[4] Elvio Bonisoli, Nicoló Manca, and Maurizio Repetto. Multi-physics optimisation of energy harvesters. *COMPEL: The International Journal for Computation and Mathematics in Electrical and Electronic Engineering*, 34(5):1392–1403, 2015.

[5] P Gardonio and MJ Brennan. *Mobility and impedance methods in structural dynamics*, volume 9. chapter, 2004.

[6] Aldo Romani, Rudi Paolo Paganelli, Enrico Sangiorgi, and Marco Tartagni. Joint modeling of piezoelectric transducers and power conversion circuits for energy harvesting applications. *IEEE Sensors Journal*, 13(3):916–925, 2013.